Selective stacking in the reflection-angle and azimuth domain

Yaxun Tang, Stanford University*

SUMMARY

I analytically demonstrate the artifacts in angle-domain common-image gathers caused by sparsely sampled wavefields, from a perspective of shot-profile migration. The local-offset gather is linearly related to the angle gather in locally constant-velocity media when wavefields are sufficiently well sampled, but not when wavefields are poorly sampled. Hence, linear slant-stack or radial-trace transform in local-offset gathers will produce angle gathers with artifacts, which may hinder further interpretation or analysis and reduce the quality of the final stacking image in the angle and azimuth domain. Instead of simply stacking along reflection angle and azimuth axes, I present a method to compute the stacking weights as functions of angle and azimuth and make the stacking process selective. My method is tested on the synthetic wide-azimuth version of the SEG/EAGE salt data set, where a cleaner image with higher signal-to-noise ratio is obtained.

INTRODUCTION

Seismic image quality is highly dependent on the acquisition geometry, or more specifically, on the illumination of the subsurface. Ideally, the best image is obtained when each subsurface image point is illuminated equally, which potentially requires an infinite recording geometry. In the real world, however, we always have a limited recording geometry, like in the marine-streamer acquisition system, where only narrow-azimuth data are acquired. Recent developments in multi-azimuth or wide-azimuth acquistion techniques (Michell et al., 2006; Keggin et al., 2006; Howard and Moldoveanu, 2006) provide us richer coverage in azimuth, and the subsurface can be better illuminated, especially in subsalt areas. Much better images are obtained because of improved subsurface illumination. Nevertheless, the reality can never meet the requirement for infinite recording geometry and infinitly dense sampling for shots and receivers. Shadow zones or illumination holes and aliases may still happen in complex geologies. Poor illumination results in poor images, and related artifacts destort the migrated image, making it difficult to interpret. This effect is readily visible in the reflection-angle and azimuth domain, where illumination holes and related artifacts can be identified. They are by no means random or weak, and thus simple stacking can not attenuate them effectively.

In this paper, I briefly review methods for extracting subsurface-offset-domain common-image gathers (SODCIGs) and angle-domain common-image gathers (ADCIGs). I demonstrate the effects of sparsely sampled wavefields on both SODCIGs and ADCIGs. I also demonstrate that the final image formed by simple stacking over the reflection-angle and azimuth axes without any weighting function suffers from artifacts caused by poor illumination and has a low signal-to-noise ratio. Instead, I describe a simple but effective way to make the stacking process selective: we stack only those reflection angles and azimuths with good illumination. This method is tested on the wide-azimuth version of the SEG/EAGE salt data set, and a better image with higher signal-to-noise ratio is obtained.

EXTRACTING ANGLE-DOMAIN COMMON-IMAGE GATHERS

ADCIGs can be extracted either before applying an imaging condition (Prucha and Symes, 1999; Mosher and Foster, 2000; Xie and Wu, 2002; Soubaras, 2003) or afterward (Sava and Fomel, 2003; Biondi and Symes, 2004). The advantage of extracting the angle gathers after the imaging step is that it is a model-space processing, which offers more versatility. The same transformation can be used for images produced by source-receiver migration (Sava and Fomel, 2003), shot-profile migration (Rickett and Sava, 2002) and reverse time migration (Biondi and Shan, 2002).

There are basically two steps to extract the angle gathers after imaging: First, compute the SODCIGs. Second, transform the SODCIGs into ADCIGs. For source-receiver migration, the SODCIGs are immediately available after downward continuation of the wavefields; for shot-profile migration, a multi-offset imaging condition should be applied to get the SODCIGs (Rickett and Sava, 2002):

$$I(x,y,h_x,h_y)=\sum_{\omega} D^*(x-h_x,y-h_y,\omega)U(x+h_x,y+h_y,\omega), \tag{1}$$

where I is the image in the subsurface-offset domain, D is the source wavefield, * means the conjugate, U is the receiver wavefield, x, y are the components of midpoint and h_x, h_y are the components of subsurface half offset, and ω is frequency. Sava and Fomel (2003) derived the following radial-trace transformation in the Fourier domain to transform the SODCIGs into ADCIGs in 2-D:

$$\tan\gamma=-\frac{k_{h_x}}{k_z}=-\frac{\partial z}{\partial h_x}, \tag{2}$$

where γ is the reflection angle, k_{h_x} is the offset wavenumber, and k_z is the depth wavenumber. The transformation is independent of geological dip in 2-D, but the 3-D formulation must be corrected for a crossline dip component. Tisserant and Biondi (2003) show that we can make this 3-D correction by re-writing the angle-gather transformation as

$$\tan\gamma=-\frac{|\mathbf{k_h}|}{k_z}\frac{1}{\sqrt{1+\left(\frac{k_{m_x}}{k_z}\sin\beta+\frac{k_{m_y}}{k_z}\cos\beta\right)^2}}, \tag{3}$$

where β is the reflection azimuth, $|\mathbf{k_h}|$ is the absolute value of the offset wavenumber, k_{m_x} and k_{m_y} are the components of the midpoint wavenumber.

ARTIFACTS CAUSED BY SPARSELY SAMPLED WAVEFIELDS

As demonstrated in Rickett and Sava (2002), ADCIGs suffer from poor sampling of the source or receiver wavefield, and the resulting artifacts ruin the quality of the angle gathers, making interpretation, AVA analysis and velocity prediction difficult. This effect is not very obvious from the derivation in Sava and Fomel (2003); it is, however, more evident from the perspective of shot-profile migration. It can be analytically demonstrated that in locally constant-velocity media, when the receiver wavefield is densely sampled, the circular wavefronts of the downward continued receiver wavefields can be well reconstructed, as shown in Figure 1; hence the multi-offset imaging condition in equation (1) produces a linear relationship between local offset h_x and depth z for a specific CMP location x as follows (Tang, 2007):

$$z=-\tan\alpha x-\tan\gamma h_x, \tag{4}$$

where α is the geological dip and γ is the reflection angle. If we take the derivative of z with respect to h_x, we get

$$\tan\gamma=-\frac{\partial z}{\partial h_x}=-\frac{k_{h_x}}{k_z}, \tag{5}$$

which is exactly the same as equation (2). In other words, for well-sampled receiver wavefields, one shot will generate local-offset gathers with a straight line. The slope of that line in local-offset domain is the tangent of the reflection angle γ. Hence, radial-trace or slant-stack transform in the local-offset domain will produce artifact-free angle gathers, and a straight line in local-offset gathers would be strictly mapped to a single point in the ADCIGs.

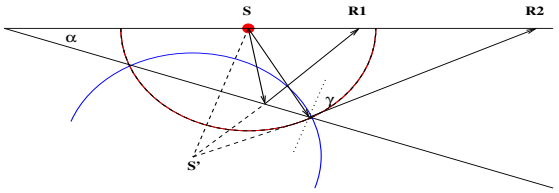

Figure 1: When the receiver wavefield is sufficiently densely sampled, the actual circular wavefront in blue can be well recontructed.

Let us consider the extreme case for poor sampling, where we have only one receiver, as shown in Figure 2. It can also be analytically demonstrated that, when we have only one shot and one receiver, the multi-offset imaging condition in equation (1) no longer produces a linear relationship between local offset h_x and depth z. Instead z and h_x are non-linearly related as follows (Tang, 2007):

$$z^2 = -h_x^2 + (r-s)h_x + \frac{(r-s)^2}{\left[\tan(-\gamma-\alpha)+\tan(-\gamma+\alpha)\right]^2}, \quad (6)$$

where s and r are the source location and receiver location respectively, and α is the geological dip. In such situations, the linear transformation from the local-offset domain to angle domain will definitely produce unwanted artifacts. Note that though here I limit my discussion to the effect in ADCIGs caused by poorly sampled receiver wavefields, reciprocity implies that the same should be true for poorly sampled source wavefields.

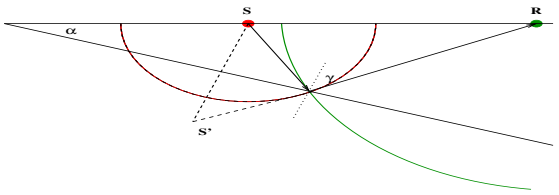

Figure 2: In the extreme situation where there is only one receiver, the receiver wavefront is the one shown in green, instead of the blue onw shown in Figure 1.

For example, I generate a synthetic shot gather for a flat reflector at $z = 2000$ meters, with a constant velocity $v = 4000$ m/s. The shot is located at $x = -1000$ meters, the receivers are ranging from -16000 meters to 14000 meters on the surface with a spacing equals 10 meters. For an image point at $(x = 0, z = 2000)$, the reflection angle should be $\gamma = \arctan(1000/2000) = 26.6°$. Figure 3(a) shows the SODCIG or local-offset gather at surface location $x = 0$ obtained by migrating all the receivers; it shows a perfectly straight line intersecting at $(0, 2000)$ in the local-offset domain (h_x, z). Figure 3(c) shows the ADCIG obtained by slant-stacking the corresponding SODCIGs in Figure 3(a). This result also shows a nice point located at about 26.6°, which matches the theoretical result well. Figure 3(b) shows the SODCIG at $x = 0$ meter obtained by migrating with only one receiver located at $x = 1000$ meters. As predicted by equation (6), it is a circle instead of a straight line intersecting at $(0, 2000)$ in the local-offset domain (h_x, z). The corresponding ADCIG is shown in Figure 3(d). Instead of a nicely focused point at 26.6°, we can identify a downward-frowning curve.

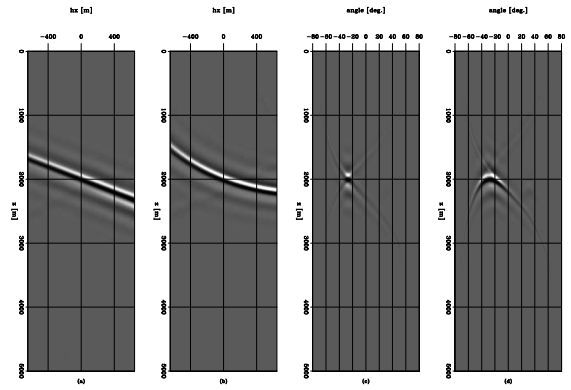

Figure 3: SODCIGs and ADCIGs at $x = 0$ meter for different results. (a) SODCIG obtained by migrating all the receivers, where a straight line is obtained, since the receiver wavefield is well sampled. (b) SODCIG obtained by migrating only one receiver located at $x = 1000$ meters, where a circle instead of a straight line is obtained, since the wavefield is extremely poorly sampled. (c) ADCIG computed from (a), where a nicely focused point at 26.6° is obtained, because the local-offset gather in (a) is linear. (d) ADCIG computed from (b), where a downward-frowning curve instead of a point is obtained, because the local-offset gather in (b) is non-linear.

SELECTIVE STACKING BASED ON LOCAL SMOOTHING OF THE ENVELOPE FUNCTION

The downward-frowning artifacts observed in the previous section have a great influence on seismic angle-domain processing. They can destort the final image when we stack over the angle and azimuth axes, generating fake reflectors that can lead to misinterpretation. They can also affect the accuracy of residual-moveout-based velocity analysis, since with those frowning curves, it is difficult to predict the residual moveout acurately. There are four possible methods to get rid of those artifacts in angle gathers:

1. Define a non-linear transformation in the local-offset domain to get an artifact-free angle gather.

2. Densely interpolate the data before migration. This data-space interpolation is very helpful if the underground velocity structure is simple, but helps little or not at all if the velocity structure is complex.

3. Apply image-space interpolation. By assuming that reflectivities are changing smoothly along angles and azimuths and that any abrupt changes in amplitudes are caused by poor illumination or poor sampling, we can run least-squares inversion with regularization in the angle domain by smoothing along angles and azimuths to attenuate those artifacts (Prucha et al., 2000). Or equivalently, we can run least-squares inversion with differential-semblence regularization in the subsurface-offset domain (Valenciano, 2006; Tang, 2006). Both these methods are effective but computationally demanding.

4. Apply selective stacking by designing filters or weighting functions that ignore those artifacts, stacking only angles and azimuths with good illumination and dense sampling.

In this paper, I will concentrate mainly on the fourth method and describe a simple but effective way to design the weighting functions. As we know, when migrating with the correct migration velocity and with densely sampled and infinite recording geometry, the events in ADCIGs are aligned horizontally. In 2-D there are horizontal lines in the angle domain; in 3-D there are flat planes in the angle and azimuth domain, because with infinite acquisition geometry, all angles and azimuths should be illuminated. When we don't have densely sampled and infinite recording geometry, there are holes in the line in the 2-D case or holes in the plane in the 3-D case. The shape of holes can be fairly irregular, depending on the recording geometry and the geological structure of the subsurface. The goal of the method is to attenuate the artifacts and enhance the signal-to-noise ratio of the final image by stacking only those angles and azimuths that are well illuminated. I first compute the envelope of the 3-D angle gather, then apply 3-D local smoothing based on equation (7) to the computed envelope to get the weighting function,

$$W(z,\gamma,\beta) = \frac{1}{2L+1}\sum_{j=-L}^{L} s(j)E(z+j\Delta z,\gamma+j\Delta\gamma,\theta+j\Delta\beta), \tag{7}$$

where W and E are the weighting function and envelope function respectively for a particular CMP location. They are functions of depth z, reflection angle γ and reflection azimuth β. L is the half length of the moving window, and $s(j)$ determines the shape of the smoothing operator. In this paper I use a 3-D local boxcar smoothing operator, so $s(j) = 1$. A more sophisticated smoothing operator, such as a 3-D local Gaussian smoothing operator, could also be applied.

3-D SEG/EAGE SALT MODEL EXAMPLE

I test the method discussed above on the 3-D wide-azimuth version of the SEG/EAGE salt data set. The wide-azimuth synthetic data is from Sandia National Laboratory, which has 45 shots in total, with a shot interval of about 960 meters in both the inline and crossline directions. The receiver geometry is a patching geometry, with minumum offset of about -2000 meters and maximum offset of about 2000 meters in both the inline and crossline directions.

The migrated image obtained by using shot-profile migration for all 45 shots is shown in Figure 4. The left panel in Figure 5 illustrates the SODCIG at surface location $(8200, 8840)$, from which we can see that since the correct migration velocity is used, there is some focusing of energy at zero offset. However, the energy is not well focused because there are only 45 shots, and thus at most 45 planes intersecting at zero-offset location, which are not sufficient to cancel the energy at non-zero offsets.

Since the sources are extremely sparsely located, and the receiver coverage is limited for each shot, we can identify some curvatures in the SODCIGs shown in the left panel in Figure 5. For the events above the salt, the curvatures are not very obvious, because the velocity model above the salt is relatively simple; however, we can still see that some of the events are bending at far offsets. For events that are below the salt, the curvatures are more obvious, because with the complex salt body and limited recording geometry, it is impossible to have the receiver wavefield well sampled.

SODCIGs are transformed into 3-D ADCIGs by using equation (3). The corresponding ADCIG is shown in the right panel in Figure 5, where the vertical axis is depth, the inline axis is reflection angle and the crossline axis is reflection azimuth. The computed azimuth range is from 0 to 180 degrees with a spacing of 5 degrees. Note the blobs in the depth slices, which are closely related to the shot locations.

As demonstrated in the previous section, linear transformation from

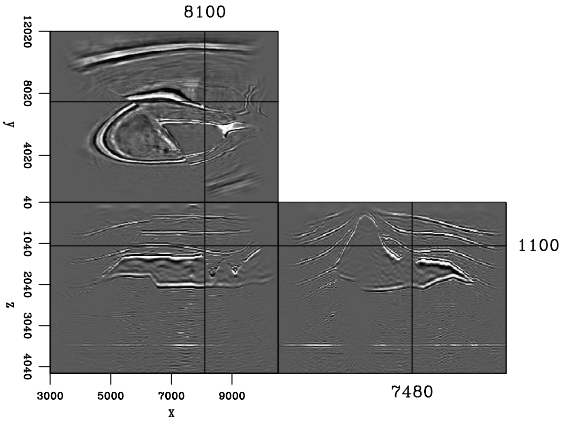

Figure 4: Shot-profile migration result of all 45 shots.

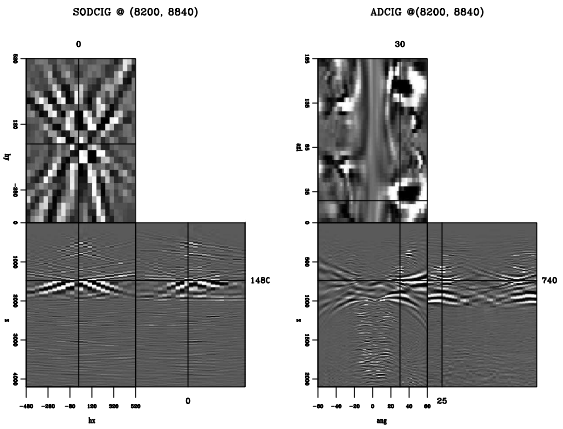

Figure 5: SODCIGs and ADCIGs for surface location $(8200, 8840)$ The left panel shows the SODCIG, where the vertical axis is depth, the inline axis is h_x and the crossline axis is h_y. The right panel shows the ADCIG, where the vertical axis is depth, the inline axis is reflection angle and the crossline axis is reflection azimuth.

SODCIGs to ADCIGs is prone to artifacts when the source or receiver wavefield is poorly sampled (sparsely distributed shot locations or receiver locations). Another possible reason for artifacts is large velocity contrast in the vicinity of the image point, since the equations for local-offset to angle transformation are valid only in media with locally constant velocity. Artifacts can be easily identified in ADCIGs for SEG/EAGE salt model as shown in the right panel in Figure 5. We can find smeared energy (tails) in both near angles and far angles, especially in the top salt and base salt areas, where the velocity contrast is high, and in the subsalt area, where the wavefields are poorly sampled.

To form the final image cube, we have to stack the ADCIGs along both the reflection-angle and reflection-azimuth axes. As the transformation artifacts are not random, simple stacking without any weighting function might produce images with low signal-to-noise ratios, making interpretation difficult. The simply stacked image, shown in Figure 7(c), is quite noisy, especially in the subsalt. It is definitely difficult to interpret.

Instead of simply stacking along the angle and azimuth axes, we can apply weighting functions which attenuate unwanted artifacts

to make the stacking process selective. The weighting functions are computed by using equation (7). Figure 6(b) shows the weighting function for the image point at (8200, 8840). We can see that horizontally incoherent energy at near and far angles receives low weights, while horizontally coherent energy, where the actual reflection is located, receives high weights. Figure 6(c) shows the filtered result, in which the artifacts are greatly suppressed.

The weighting functions are computed for every image point and applied to the original ADCIGs, then the filtered ADCIGs are stacked together to form the final image. Figure 7(d) shows the result of using this kind of selective stacking. For comparison, Figure 7(a) shows the corresponding velocity model, Figure 7(b) shows the zero-offset image extracted from the SODCIG cube with $h_x = 0$ and $h_y = 0$, and Figure 7(c) shows the image obtained by simply stacking the ADCIGs without any weighting functions. It is quite obvious that the image in Figure 7(d) obtained by using selective stacking, has the highest signal-to-noise ratio and it is the cleanest among the three. Also notice the migration artifacts at the bottom of the image, which can be easily identified in Figures 7(b) and (c), but are greatly attenuated in Figure 7(d). The dipping reflector under the salt on the side panel, which is nearly invisible in Figure 7(b) and noisy in Figure 7(c), is clearly visible in Figure 7(d).

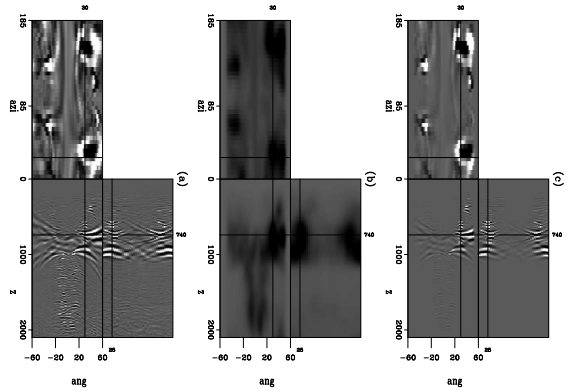

Figure 6: Filtering result for ADCIG at (8200, 8840). Panel (a) shows the original ADCIG, (b) is the computed weighting function via local smoothing of the envelope function, where dark color stands for high weight and light color stands for low weight. Panel (c) is (a) multiplied with (b), i.e. the filtered ADCIG.

CONCLUSION

I analytically demonstrated that when source or receiver wavefields are poorly sampled, subsurface or local-offset gathers are no longer linearly related to angle gathers. Slant-stack or radial-trace transform is prone to artifacts in such situations. This often happens when the underground velocity structure is very complex, since in complex geologies with limited recording geometries, it is difficult to have wavefields well sampled. To eliminate those artifacts, I presented a selective-stacking approach based on local smoothing of the envelope function. My test on the complex SEG/EAGE salt data set shows that by selectively stacking in the reflection angle and azimuth domain, a cleaner image with higher signal-to-noise ratio and less migration artifacts can be obtained.

ACKNOWLEDGMENTS

The author would like to thank the sponsors of the Stanford Exploration Project for their financial support.

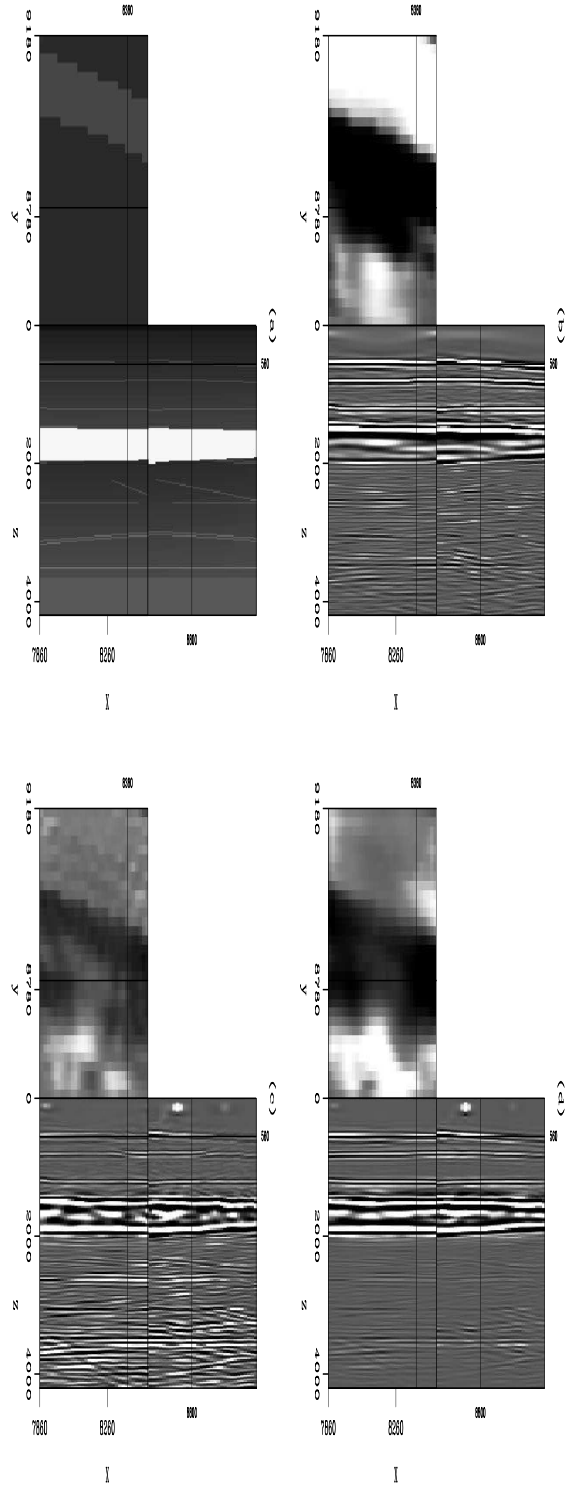

Figure 7: Comparison for different results. Panel (a) is the corresponding velocity model; (b) is the zero-offset image extracted from the SODCIG cube with $h_x = 0$ and $h_y = 0$; (c) is the result obtained by simple stacking without any weighting function; and (d) is the result obtained by selective stacking, with the weighting function computed by locally smoothing the envelope function of the ADCIGs.

EDITED REFERENCES

Note: This reference list is a copy-edited version of the reference list submitted by the author. Reference lists for the 2007 SEG Technical Program Expanded Abstracts have been copy edited so that references provided with the online metadata for each paper will achieve a high degree of linking to cited sources that appear on the Web.

REFERENCES

Biondi, B., and G. Shan, 2002, Prestack imaging of overturned reflections by reverse time migration: 72nd Annual International Meeting, SEG, Expanded Abstracts, 1284–1287.

Biondi, B., and W. Symes, 2004, Angle-domain commonimage gathers for migration velocity analysis by wavefield-continuation imaging: Geophysics, 69, 1283–1298.

Howard, M. S., and N. Moldoveanu, 2006, Marine survey design for rich-azimuth seismic using surface streamers: 76th Annual International Meeting, SEG, Expanded Abstracts, 2915–2919.

Keggin, J., T. Manning, W. Rietveld, C. Page, E. Fromyr, and R. van Borselen, 2006, Key aspects of multi-azimuth acquisition and processing: 76th Annual International Meeting, SEG, Expanded Abstracts, 2886–2890.

Michell, S., E. Shoshitaishvili, D. Chergotis, J. Sharp, and J. Etgen, 2006, Wide azimuth streamer imaging of mad dog: Have we solved the subsalt imaging problem?: 76th Annual International Meeting, SEG, Expanded Abstracts, 2905–2909.

Mosher, C., and D. Foster, 2000, Common angle imaging conditions for prestack depth migration: 70th Annual International Meeting, SEG, Expanded Abstracts, 830–833.

Prucha, B. B., and W. Symes, 1999, Angle-domain common-image gathers by wave-equation migration: 69th Annual International Meeting, SEG, Expanded Abstracts, 824–827.

Prucha, M. L., R. G. Clapp, and B. Biondi, 2000, Seismic image regularization in the reflection angle domain: SEP-103, 109–119.

Rickett, J. E., and P. C. Sava, 2002, Offset and angle-domain common image-point gathers for shot-profile migration: Geophysics, 67, 883–889.

Sava, P. C., and S. Fomel, 2003, Angle-domain common-image gathers by wavefield continuation methods: Geophysics, 68, 1065–1074.

Soubaras, R., 2003, Angle gathers for shot-record migration by local harmonic decomposition: 73rd Annual International Meeting, SEG, Expanded Abstracts, 889–892.

Tang, Y., 2006, Least-squares migration of incomplete data sets with regularization in the subsurface-offset domain: SEP-125, 159–174.

———, 2007, Selective stacking in the reflection-angle and azimuth domain: SEP-129.

Tisserant, T., and B. Biondi, 2003, Wavefield-continuation angle-domain common-image gathers in 3-D: SEP-113, 211–220.

Valenciano, A. A., 2006, Target-oriented wave-equation inversion with regularization in the subsurface offset domain: SEP-124.

Xie, X., and R. Wu, 2002, Extracting angle domain information from migrated wavefield: 72nd Annual International Meeting, SEG, Expanded Abstracts, 1360–1363.